

# Double- $\mathbf{Q}$ magnetic structures and strong planar anisotropy in tetragonal $\text{ErRu}_2\text{Ge}_2$ and $\text{ErRu}_2\text{Si}_2$

 A. Garnier<sup>1</sup>, D. Gignoux<sup>1,a</sup>, B. Ouladdiaf<sup>2</sup>, D. Schmitt<sup>1</sup>, and T. Shigeoka<sup>3</sup>
<sup>1</sup> Laboratoire Louis Néel, CNRS, BP 166, 38042 Grenoble Cedex 9, France

<sup>2</sup> Institut Laue Langevin, BP 156, 38042 Grenoble Cedex 9, France

<sup>3</sup> Faculty of Science, Yamaguchi University, Yamaguchi 753, Japan

Received 24 December 1999

**Abstract.** Single crystal magnetization measurements and powder neutron diffraction on tetragonal  $\text{ErRu}_2\text{Ge}_2$  as well as anisotropy of the paramagnetic susceptibility and specific heat measurements on  $\text{ErRu}_2\text{Si}_2$  are presented. Besides the huge crystal field contribution to the uniaxial anisotropy, which favors the basal plane, a strong in-plane anisotropy is evidenced. From these features and neutron diffraction experiments it is shown that magnetic structures of these materials are double- $\mathbf{Q}$  and accordingly non-collinear below their Néel temperature (5.2 and 6.0 K for Ge and Si based compounds, respectively). The magnetic structures induced during the metamagnetic processes are discussed.

**PACS.** 75.25.+z Spin arrangements in magnetically ordered materials (including neutron and spin-polarized electron studies, synchrotron-source, x-ray scattering, etc.) – 75.30.Kz Magnetic phase boundaries (including magnetic transitions, metamagnetism, etc.) – 75.30.Gw Magnetic anisotropy

## 1 Introduction

The  $\text{RM}_2\text{X}_2$  compounds (R = rare earth, M = Mn, Fe, Co, Ni, Cu, Ru, Rh and X = Si, Ge) have been shown to belong to the large family of ternary compounds which crystallize in the well-known tetragonal  $\text{ThCr}_2\text{Si}_2$ -type structure (space group  $I4/mmm$ ) [1]. These compounds are of special interest because the frustration of magnetic interactions associated with the large uniaxial magnetocrystalline anisotropy arising from crystalline electric field (CEF) effects leads, at low temperature, to complex magnetic phase diagrams in which original properties, such as multistep metamagnetic processes, incommensurate magnetic structures, mixed magnetic structures, have been evidenced [2,3]. In a large number of these compounds the  $A_2^0$  CEF parameter characterizing the surroundings is positive. Accordingly for those with rare earths having a negative second order Stevens crystal field coefficient  $\alpha_J$ ,  $\mathbf{c}$  is the easy magnetization direction leading to Ising like systems which have been extensively studied. Much less work has been performed on the few planar ( $X - Y$  type) systems where, as expected for uniaxial compounds, the anisotropy within the plane is expected to be small. In this paper we focus on  $\text{ErRu}_2\text{Ge}_2$  and  $\text{ErRu}_2\text{Si}_2$  which belong to the latter type of material. Whereas the former compound has only been known to order antiferromagnetically at low temperature [1], more results have been obtained on the compound with Si. In the latter, below  $T_N = 6$  K

neutron diffraction reveals an antiferromagnetic structure characterized by the propagation vector  $\mathbf{Q} = (0.2, 0, 0)$  in reduced units and magnetic moments perpendicular to  $\mathbf{Q}$ , *i.e.* along  $[010]$  [4]. However, magnetic measurements on a single crystal showed that the  $\langle 110 \rangle$  axes are the easy magnetization directions [5] and it has been suggested that there is a good possibility for a double- $\mathbf{Q}$  structure.

In order to gain insight into the specificity of magnetism in these planar systems, we have studied: i)  $\text{ErRu}_2\text{Ge}_2$  by neutron diffraction on a powder and by magnetization measurement on a single crystal (Sect. 2). ii)  $\text{ErRu}_2\text{Si}_2$  by magnetization measurement on a single crystal in particular in the paramagnetic domain and by specific heat (Sect. 3). An analysis and discussion of both compounds is then presented in Section 4.

## 2 $\text{ErRu}_2\text{Ge}_2$

### 2.1 Magnetization measurements

Single crystals were grown by the Czochralski technique in an arc furnace. Magnetization was measured using the extraction technique in fields up to 10 T and in the temperature range 1.5 to 300 K. Whereas along the  $\mathbf{c}$  axis the susceptibility is very weak and does not exhibit any anomaly, along the  $[100]$  and  $[110]$  directions it is much larger and presents a well-pronounced peak at  $T_N = 5.2$  K as shown in Figure 1. Field dependences of magnetization at 1.5 K along the three symmetry directions are reported

<sup>a</sup> e-mail: gignoux@polycnrs-gre.fr

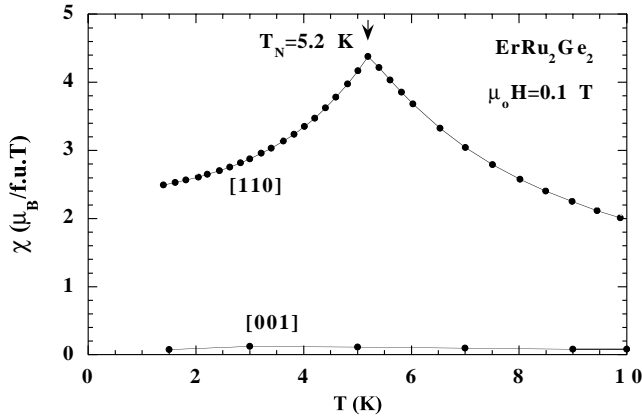


**Fig. 1.** ErRu<sub>2</sub>Ge<sub>2</sub>: low temperature thermal dependence of magnetization along the [001] and [110] axes in a  $\mu_0 H = 0.1$  T applied field. Along [001] the values reported are the experimental ones multiplied by 10.

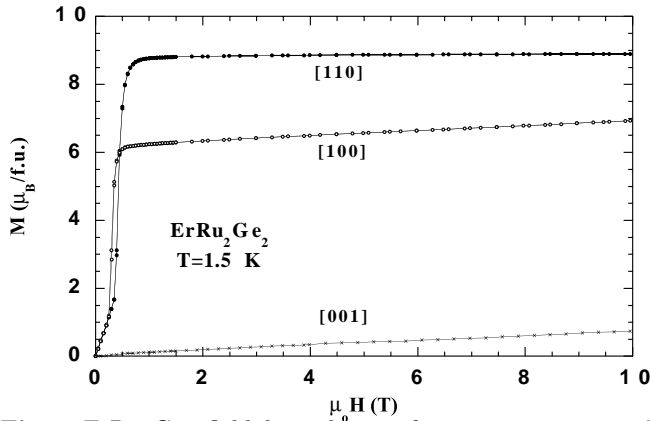


**Fig. 2.** ErRu<sub>2</sub>Ge<sub>2</sub>: field dependences of magnetization at 1.5 K along the three symmetry axes.

in Figure 2. A huge anisotropy is observed between the  $c$  axis and the basal plane. Along  $c$ , magnetization is always very weak and increases almost linearly with the field. In a 10 T applied field it reaches only  $0.74 \mu_B/f.u.$  Along [100] and [110] axes a single-step metamagnetic transition occurs at  $H_c[100] = 0.3$  T and  $H_c[110] = 0.4$  T, respectively. The hysteresis of these transitions are negligible. Note that below the transition the susceptibility is rather large and almost the same along both axes (see discussion). Above the transition, a large anisotropy is observed with the following characteristics: i) Magnetization increases weakly and almost linearly with a slope of  $0.0320$  and  $0.0802 \mu_B/f.u.T$  for [110] and [100], respectively. ii) In a 0.8 T applied field along [110], magnetization reaches  $8.70 \mu_B/f.u.$ , a value close to the free Er<sup>3+</sup> ion value ( $9.00 \mu_B$ ), showing that the magnetic structure has become ferromagnetic colinear. In the same field along [100], magnetization is  $6.21 \mu_B/f.u.$ , *i.e.* a value very close to  $8.70 \cos(45^\circ) = 6.15$ . iii) In the maximum field of 10 T,  $M$  is  $8.89 \mu_B/f.u.$  along [110] and  $6.94 \mu_B/f.u.$  along [100] ( $8.89 \cos(45^\circ) = 6.27$ ). These results clearly show that  $\langle 110 \rangle$  axes are the easy magnetization directions and that the anisotropy between these and the  $\langle 100 \rangle$  axes is very large. Indeed, even in a 10 T applied field along [100],

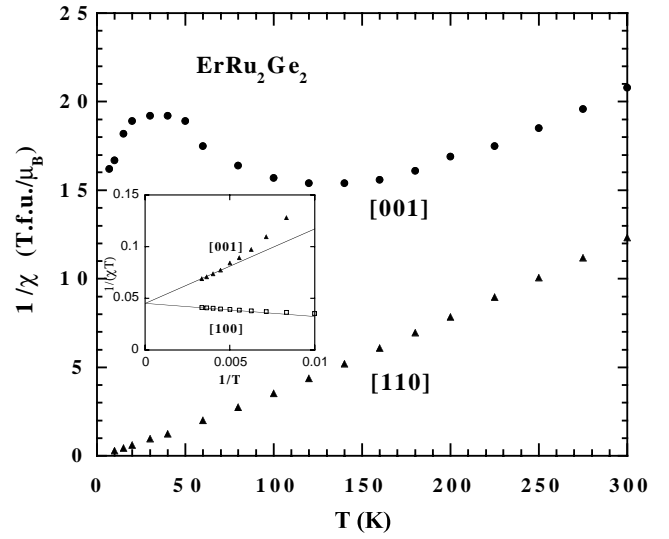


**Fig. 3.** ErRu<sub>2</sub>Ge<sub>2</sub>: thermal dependences of the reciprocal susceptibilities above the Néel temperature parallel and perpendicular to  $c$ . The inset shows  $1/(\chi T)$  vs.  $1/T$  plots for the high temperature region.

the angle between this axis and magnetic moments is still about  $39^\circ$ . When temperature is increased, the same behavior is observed, the transition becoming smoother and disappearing at  $T_N$ .

Within the paramagnetic domain the susceptibility has been deduced from the  $M^2$  vs.  $M/H$  Arrott plots. The thermal variations of the reciprocal susceptibility along and perpendicular to  $c$ , thus obtained are reported in Figure 3. Within the basal plane, the reciprocal susceptibility follows the linear Curie Weiss law above 120 K. Along [001] CEF effects are so large that the Curie Weiss law is hardly observed above 250 K. At lower temperature, experimental points strongly deviate from this law showing first a minimum around 130 K and then a large maximum around 30 K. It is then difficult and even impossible along [001] to determine from these  $1/\chi$  variations, the effective moment and the paramagnetic Curie temperatures. Therefore we used the following approach: From the high temperature Curie Weiss law ( $1/\chi = (T - \theta_p)/C$ ) one can write:

$$\frac{1}{\chi T} = \frac{1}{C} - \frac{\theta_p}{C T}.$$

Then plotting  $1/(\chi T)$  vs.  $1/T$ , we should expect a linear variations for small values of  $1/T$  with the following characteristics: i) plots along and perpendicular to [001] should have the same limit value ( $1/C$ ) for  $1/T \rightarrow 0$ , ii) the slopes allow the determination of the paramagnetic Curie temperatures. From these plots shown in the inset of Figure 3 one deduces: i) an effective moment of  $9.85 \mu_B/f.u.$ , a value in good agreement with the free Er<sup>3+</sup> ion value ( $9.60 \mu_B$ ). ii)  $\theta_p(\parallel c) = 150$  K and  $\theta_p(\perp c) = -28$  K.

## 2.2 Neutron diffraction

Neutron diffraction experiments on a powder sample were performed on the D1B spectrometer at the ILL (Grenoble)

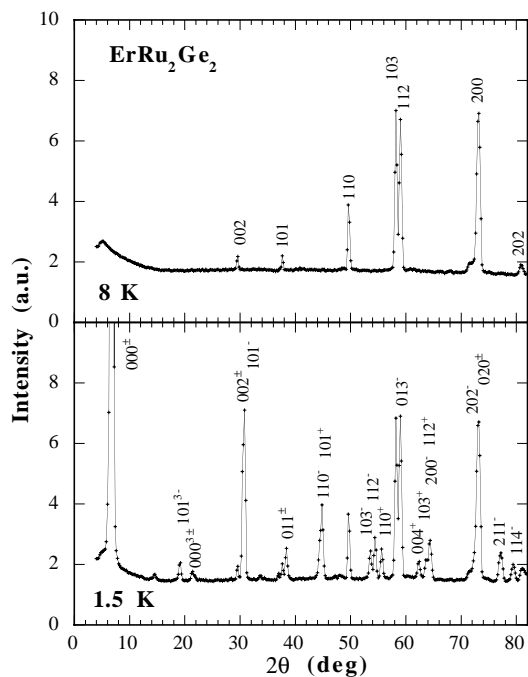


**Fig. 4.**  $\text{ErRu}_2\text{Ge}_2$ : powder neutron diffraction pattern at 1.5 K and 8 K. Peaks indexed as  $hkl^-$  or  $hkl^{3-}$  correspond to points of co-ordinates  $(h - \tau, k, l)$  or  $(h - 3\tau, k, l)$  respectively of the reciprocal space when writing  $\mathbf{Q} = (\tau, 0, 0)$ .

at different temperatures (1.5, 3, 3.5, 4 and 8 K). The wavelength was 2.522 Å. Spectra, measured out at 8 K and 1.5 K, are shown in Figure 4. At 8 K the pattern is characteristic of the crystallographic structure. However, on account of texture effects of the crystallites, the refinement of the observed intensities led to a reliability factor  $R = \sum |I_{\text{cal}} - I_{\text{obs}}| / \sum I_{\text{obs}}$  of only 12.0%. At 1.5 K additional peaks appear which can be indexed with the incommensurate propagation vector  $\mathbf{Q} = (0.211, 0, 0)$  in reduced unit. Peaks indexed as  $hkl^-$  in the figure correspond to points of co-ordinate  $(h - 0.211, k, l)$  of the reciprocal space. In particular at  $2\theta = 7.11^\circ$  the first harmonic of the origin appears very strong due to the large Lorentz factor. When the temperature is increased the propagation vector does not change for  $T$  up to  $T_N$  within the experimental accuracy. Third order harmonics are clearly observed at 1.5 K around  $20^\circ$ . They decrease rapidly when the temperature is increased and have completely disappeared at 4 K.

The neutron diffraction results can be interpreted considering either single- $\mathbf{Q}$  or double- $\mathbf{Q}$  structures. In both cases the refinement of the magnetic structure at 1.5 K leads to the same intensities for the diffraction peaks with a reliability factor  $R = 19.3\%$ . Both solutions thus appear indistinguishable when taking into account powder neutron diffraction alone.

i) Considering a colinear single- $\mathbf{Q}$  structure, magnetic moments are perpendicular to the propagation vector and along one of the two  $\langle 100 \rangle$  directions with a modulus of the first order harmonic  $M_{\mathbf{Q}}$  of  $10.1 \mu_B$  (in our formalism the component of the Er moment along one

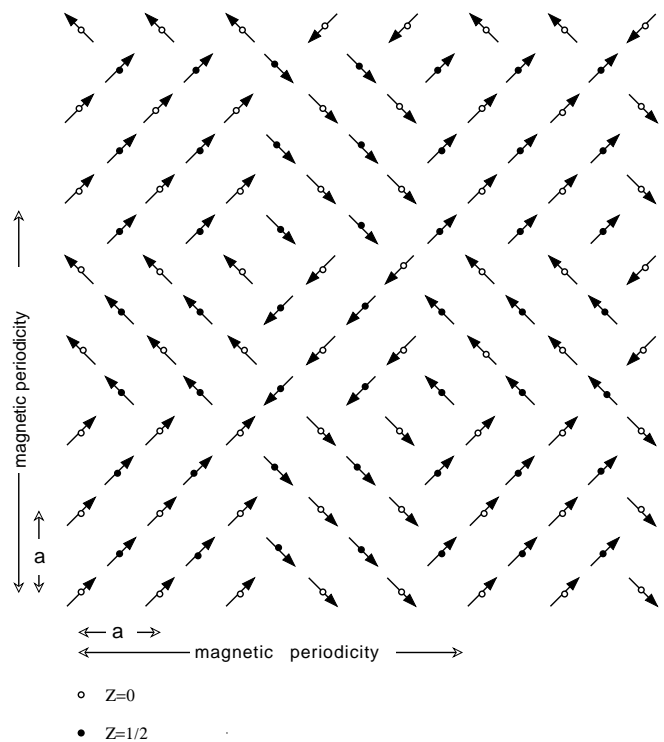


**Fig. 5.**  $\text{ErRu}_2\text{Ge}_2$ : Schematic representation of the fully antiphase magnetic structure expected at 0 K. Note that the magnetic periodicity is incommensurate with the crystallographic one.

direction is written as  $M(\mathbf{r}_i) = M_{n\mathbf{Q}} \sin(2\pi n\mathbf{Q} \cdot \mathbf{r}_i + \varphi_n)$  where  $\mathbf{r}_i$  is the position of the atom  $i$ ). Note that a (non-colinear) cycloidal structure with moments rotating within the (001) plane leads to a very bad reliability factor (36%).

ii) The double- $\mathbf{Q}$  structure results from the superposition of the single- $\mathbf{Q}$  structures (of the above type) associated with the two  $\langle 100 \rangle$  possible directions for  $\mathbf{Q}$  and  $M_{\mathbf{Q}}$ , *i.e.*  $\mathbf{Q}_1$  and  $M_{\mathbf{Q}_1}$  parallel to  $[100]$  and  $[010]$  respectively, and conversely for  $\mathbf{Q}_2$  and  $M_{\mathbf{Q}_2}$ . In that case the modulus of each  $M_{\mathbf{Q}_i}$  component is  $7.1 \mu_B$ . In this second case the magnetic structure is non colinear with moments on each site along one of the  $\langle 110 \rangle$  directions and the amplitude of the Er moment associated with the first order harmonic is  $7.1\sqrt{2} = 10.1 \mu_B$ .

The ambiguity between both structures can be lifted if one considers other experiments in particular magnetization measurements on a single crystal. The measurements clearly show that  $\langle 110 \rangle$  is the easy axis and accordingly that the magnetic structure is double- $\mathbf{Q}$  non colinear. The corresponding structure is shown in Figure 5.

The onset of third order harmonics below 4 K and the increase of their intensity when the temperature is decreased confirms a progressive squaring of the structure, *i.e.* a progressive evolution from a sine wave modulation of the moments at 4 K towards an antiphase structure where all the moments have the same amplitude. The former

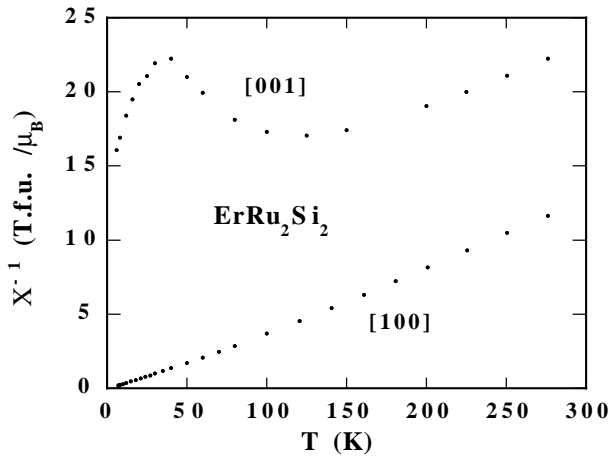


**Fig. 6.** ErRu<sub>2</sub>Si<sub>2</sub>: thermal dependences of the reciprocal susceptibilities above the Néel temperature parallel and perpendicular to *c*.

situation is characterized by the absence of peaks associated with harmonics of higher order than the first whereas the latter case is characterized by peaks associated with higher order harmonics in particular the third order with a ratio  $I(000^{\pm 3})/I(000^{\pm})$  of the intensities corrected for the Lorentz factor equal to 1/9. This is the expected situation at 0 K. At 1.5 K this ratio is half the above value showing that at this temperature the fully antiphase structure is close (indeed such a ratio means that the amplitude of the third order harmonic  $M_{3\mathbf{Q}}$  is only 0.71 that of the fully antiphase structure). This is not surprising on account of the small value of the ordering temperature. Note that for a sine wave modulation, the modulus of  $M_{\mathbf{Q}}$  is the amplitude of the moment modulation, whereas for a fully antiphase structure the amplitude of  $M_{\mathbf{Q}}$  is equal to  $4M_0/\pi$  where  $M_0$  is the value of the magnetic moment component. The determined value of  $M_{\mathbf{Q}}$  is in rather good agreement with the value of  $M_0$  which should be around the value of the magnetic moment determined from magnetic measurements just above the transition, *i.e.*  $8.7 \mu_B$ .

### 3 ErRu<sub>2</sub>Si<sub>2</sub>

#### 3.1 Magnetic measurements

Field dependences of magnetization performed along the symmetry axes of the single crystal confirmed the behavior previously observed below  $T_N = 6.0$  K characterized, as for ErRu<sub>2</sub>Ge<sub>2</sub>, by i) a huge anisotropy between this plane and the *c* axis, ii) a large anisotropy within the plane where the easy directions are the  $\langle 110 \rangle$  axes and iii) metamagnetic processes within the basal plane [5].

The thermal variations of the reciprocal susceptibility of ErRu<sub>2</sub>Si<sub>2</sub> along and perpendicular to *c*, obtained in the same way as for ErRu<sub>2</sub>Ge<sub>2</sub>, are reported in Figure 6. They present the same characteristics as those of the Ge based compound, in particular, along the [001] direction, a minimum around 130 K, and a well-pronounced maximum around 40 K due to CEF effects. As along this axis the

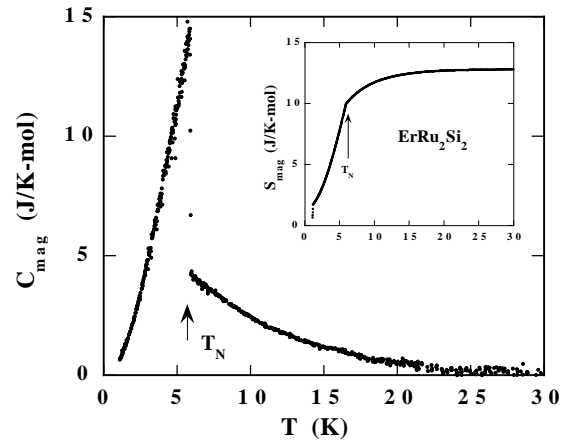


**Fig. 7.** ErRu<sub>2</sub>Si<sub>2</sub>: thermal dependence of the low temperature magnetic contribution to the specific heat. The inset shows the deduced magnetic entropy.

Curie Weiss law is hardly followed at high temperature, the Curie constant and the paramagnetic Curie temperatures were determined in the same way as for the Ge compound. The same effective moment of  $9.85 \mu_B/\text{f.u.}$  is obtained, whereas  $\theta_p(\parallel c) = 197$  K and  $\theta_p(\perp c) = -26$  K.

#### 3.2 Specific heat

The specific heat of ErRu<sub>2</sub>Si<sub>2</sub> has been measured using the alternative current method, in the temperature range 1.5–50 K. The magnetic contribution shown in Figure 7 up to 30 K, has been obtained by using the specific heat of LaRu<sub>2</sub>Si<sub>2</sub> as a phonon reference after renormalization of the Debye temperature. A unique and well-defined  $\lambda$ -type anomaly is observed at  $T_N = 6.0$  K. Above this temperature the initially high specific heat rapidly decreases and becomes very small above 25 K. This feature can be due to the high temperature tail of a Schottky anomaly centered around a few Kelvin. Magnetic fluctuations seem to be absent on account of the sharpness of the right-hand side of the  $\lambda$ -anomaly, which is sharper than that observed on other compounds of the series. It can then be deduced that the first excited state is located around 12 K above the ground state. The magnetic entropy then deduced is reported in the inset of Figure 7. It reaches  $R \ln(3)$  and  $R \ln(4)$  at  $T_N$  and 20 K, respectively. Two CEF doublets are then occupied at this latter temperature. Above 20 K the entropy tends to saturate. The other excited levels (12 doublets) are then more likely at a much higher energy as suggested by the huge magnetocrystalline anisotropy observed in this compound.

### 4 Analysis and discussion

The present study associated with previous works has shown very similar properties of ErRu<sub>2</sub>Ge<sub>2</sub> and ErRu<sub>2</sub>Si<sub>2</sub>.

Magnetization measurements on ErRu<sub>2</sub>Ge<sub>2</sub> and ErRu<sub>2</sub>Si<sub>2</sub> single crystals have evidenced the large magnetocrystalline anisotropy due to the crystal field in these

**Table 1.** Second order CEF parameters in some  $\text{RRu}_2\text{X}_2$  compounds ( $B_2^0 = \alpha_J \langle r^2 \rangle A_2^0$ ). For all the compounds we have deduced the given values using the same approach as that described for the Er-based compounds in this work.

Compound	$B_2^0$ (K)	$A_2^0$ (K)
$\text{NdRu}_2\text{Ge}_2$	-7.71	1198
$\text{TbRu}_2\text{Ge}_2$	-9.74	1272
$\text{DyRu}_2\text{Ge}_2$	-5.81	1260
$\text{ErRu}_2\text{Ge}_2$	2.34	1385
$\text{TbRu}_2\text{Si}_2$	-10.10	1319
$\text{DyRu}_2\text{Si}_2$	-4.94	1071
$\text{ErRu}_2\text{Si}_2$	2.95	1745

series. Specific heat measurements revealed information about the low lying CEF levels: in  $\text{ErRu}_2\text{Si}_2$  there are two doublets rather close together and well-separated from the higher levels, in particular at 20 K only 4 of the 16 energy levels are occupied. The anisotropy has two main features.

- (i) First the huge anisotropy already observed in the other compounds of the series is confirmed. This anisotropy mainly arises from the second order CEF term. In Table 1 we have compared the second order parameters of different compounds of both series determined in the same way. The  $A_2^0$  parameters, which characterize the surroundings, are all of the same order of magnitude with the largest values in the Er compounds. They are among the largest never observed in uniaxial materials. In particular they are much larger than in the hexagonal  $\text{RNi}_5$  [3] and  $\text{RCo}_5$  series. In  $\text{ErRu}_2\text{Si}_2$ , this parameter, if considered alone, would lead to an overall CEF splitting close to 500 K.
- (ii) The second feature is the very large anisotropy observed within the basal plane. This property had not been evidenced before because most of the deeply studied compounds of these series are of the easy **c** axis type. Such a strong anisotropy, not observed in hexagonal rare earth compounds, should mainly originate from the  $A_4^4$  and to a lesser extent  $A_6^4$  CEF parameters, whereas in hexagonal symmetry the anisotropy within the plane is only due to the  $A_6^6$  of higher order. In fact such a large planar anisotropy is also present in other series of tetragonal rare earth compounds such as the  $\text{RNi}_2\text{B}_2\text{C}$  [6] and the  $\text{RAgSb}_2$  [7] series.

The analysis of the neutron diffraction experiments and of the magnetization measurements proved that the  $\text{ErRu}_2\text{Ge}_2$  compound presents, below its Néel temperature, a non-colinear double-**Q** magnetic structure, with magnetic moments lying along the two equivalent  $\langle 110 \rangle$  directions of the basal plane. In  $\text{ErRu}_2\text{Si}_2$  the same conclusion can be made on account of the similitude of the

magnetic properties (neutron diffraction results and magnetization measurements on single crystal) with those of the Ge based compound. One remark can be made about the magnetic structure above the critical field of the metamagnetic process. When the field is along  $[110]$  it is clear that the induced state is ferromagnetic colinear, but when the field is along  $[100]$  the structure remains non-colinear; moments are equally distributed along both the  $\langle 110 \rangle$  axes with a positive component parallel to the applied field. This structure is of smaller energy than a colinear structure because it better satisfies negative interactions. Such a statement is based on the fact that the critical field along  $[100]$  is smaller than along  $[110]$  whereas it would be larger (see Sect. 2.1) for a colinear induced structure. This is confirmed by the magnetization measurements performed on  $\text{ErRu}_2\text{Si}_2$  when the field is applied in a direction intermediate between the  $[100]$  and  $[110]$  axes [5]: indeed a second transition is observed which should correspond to the change from the non-colinear ferromagnetic induced state towards a colinear state, magnetic moments remaining along or very close to the  $\langle 110 \rangle$  directions. This is rather similar to the well studied situation occurring in several compounds of the tetragonal  $\text{RNi}_2\text{B}_2\text{C}$  [6, 8] and the  $\text{RAgSb}_2$  [7] series. Further magnetic measurements are performed in order to gain a better insight into the phase diagrams (in terms of amplitude and direction of the applied field) of the compounds under investigation.

Finally it should be noticed that propagation vectors of  $\text{RRu}_2\text{X}_2$  ( $\text{X} = \text{Si}, \text{Ge}$ ) for heavy rare earths have close values (around 0.2) [3] showing that their electronic structures are very similar.

## References

1. A. Szytula, in *Handbook of Magnetic Materials*, edited by K.H.J. Buschow (North Holland, 1991), Vol. 6, pp. 85-180.
2. D. Gignoux, D. Schmitt, in *Handbook of the Physics and Chemistry of Rare Earths*, edited by K.A. Gschneidner Jr, L. Eyrings (Elsevier Science, 1995), Vol. 20, Chap. 138, pp. 293-424.
3. D. Gignoux, D. Schmitt, in *Handbook of Magnetic Materials*, edited by K.H.J. Buschow (North Holland, 1997), Vol. 10, pp. 239-414.
4. A. Blaise, R. Kmiec, B. Malaman, E. Ressouche, J.P. Sanchez, K. Tomala, G. Venturini, *J. Magn. Magn. Mater.* **135**, 171 (1994).
5. T. Takeuchi, J. Kohyama, S. Kawarazaki, M. Sato, Y. Miyako, *J. Magn. Magn. Mater.* **177-181**, 1081 (1998).
6. P.C. Canfield, S.L. Bud'ko, B.K. Cho, A. Lacerda, D. Farrell, E. Johnston-Halperin, V.A. Kalatsky, V.L. Pokrovsky, *Phys. Rev. B* **55**, 970 (1997).
7. K.D. Myers, P.C. Canfield, V.A. Kalatsky, V.L. Pokrovsky, *Phys. Rev. B* **59**, 1121 (1999).
8. P.C. Canfield, S.L. Bud'ko, *J. Alloys Comp.* **262-263**, 169 (1997).